

# Large-Scale Aligned Carbon Nanotubes from Their Purified, Highly Concentrated Suspension

Luhua Lu<sup>†,\*</sup> and Wei Chen<sup>†,\*</sup>

<sup>†</sup>Suzhou Institute of Nano-tech and Nano-bionics, Chinese Academy of Sciences, Suzhou 215125, Jiangsu, People's Republic of China, and <sup>‡</sup>Graduate University of Chinese Academy of Sciences, Beijing 100049, People's Republic of China

**ABSTRACT** Large-scale aligned single-walled carbon nanotube (SWCNT) composite membranes have been successfully prepared from highly concentrated purified SWCNT suspensions. Biopolymer dispersant gellan gum was used to achieve aqueous dispersion of highly concentrated SWCNTs, which can be used to form the SWCNT liquid crystal phase. To achieve alignment of SWCNTs, purification of SWCNTs is found to be very important. Purification was achieved by a facile and nondestructive physical method that can prepare large volumes of SWCNTs in high yield for experimental use. Composite membranes of aligned SWCNTs could be obtained by simple evaporation SWCNT liquid crystal. The orientation direction of aligned SWCNTs was controlled by mechanical shearing of SWCNT liquid crystal. The aligned SWCNTs in the biopolymer matrix were observed by electron microscopy, and the anisotropic electrical performance of this composite thin film has been characterized.

**KEYWORDS:** SWCNT alignment · purification · gellan gum · high concentration · liquid crystal

Aligned carbon nanotube (CNT) arrays have shown excellent electrical, electrochemical, and electromechanical properties compared to that of disordered CNTs.<sup>1–3</sup> However, large-scale as-grown aligned CNT arrays are hard to obtain, which seriously limits the realization of their full potential. In recent years, aligning CNTs by processing disordered CNTs<sup>4–9</sup> with external forces, such as electrical force, mechanical force, and liquid flow, has been widely studied. In this field, we have<sup>10</sup> explored the method of aligning CNTs in polyurethane by solvent–polymer interaction. Using this method, the Young's modulus of composite material has been obviously increased, but the weight fraction of CNTs is so low that the electrical and electrochemical properties of composite materials cannot reach the demands of sensors<sup>11–13</sup> and actuators.<sup>14–16</sup>

To obtain aligned CNT materials with high electrical and electrochemical performance, liquid crystal phase of highly concentrated CNT suspensions has been found<sup>17,18</sup> to be a promising method and has already been used to prepare fibrous materials.<sup>19</sup> As we know, biopolymers<sup>20,21</sup> are excellent dispers-

ants for single-walled CNTs (SWCNTs) in aqueous solution. The low mass ratio of biopolymers to SWCNTs for stable dispersion favors the preparation of highly concentrated SWCNT suspension from which the liquid crystal phase could be formed.<sup>22,23</sup> However, recently published work<sup>24</sup> has shown that the alignment of SWCNTs in such a composite material is too low to be detected by electron microscopy. There are several possible factors<sup>25</sup> that could hinder the alignment of CNTs, including the existence of spherical impurities, entanglement of CNTs, and aspect ratio of CNTs or CNT bundles. However, the influences of those possible factors have not been experimentally studied.

Here, we report our recent progress on preparing composite material of large-scale aligned SWCNTs from a highly concentrated SWCNT suspension. The biopolymer gellan gum was used to prepare a highly concentrated SWCNT aqueous suspension at low mass ratio of biopolymer to SWCNTs. The removal of spherical impurities from SWCNTs has been found to be a very important factor in achieving SWCNT alignment. Through a simple shearing treatment, the aligned SWCNT composite shows anisotropic macroscopic electrical performance.

## RESULTS AND DISCUSSION

Gellan gum has been shown to be a good agent for dispersing and stabilizing SWCNTs in aqueous solution by non-covalent polymer wrapping. The mass ratio of gellan gum to SWCNTs for dispersion is lower than widely used surfactants such as sodium dodecyl sulfate and sodium lauryl benzenesulfate.<sup>26,27</sup> In our experiment, the ideal mass ratio of

\*Address correspondence to wchen2006@sinano.ac.cn.

Received for review September 29, 2009 and accepted January 12, 2010.

Published online January 20, 2010.  
10.1021/nn901326m

© 2010 American Chemical Society

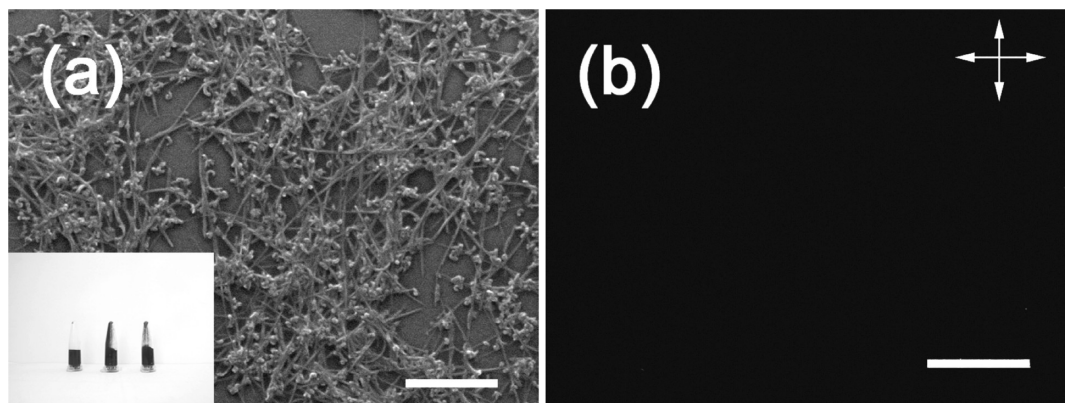


**Figure 1.** Field emission scanning electron microscope (FESEM) image for (a) SWCNTs dispersed at a mass ratio of 20:50 to gellan gum, scale bar 500 nm; inset image is the photograph of 15 min high speed centrifuged SWCNT suspensions of initial mass ratio (from left to right) of 20:50, 15:50, and 10:50 for gellan gum to SWCNTs; (b) bireflection image of suspension containing 50 mg/mL SWCNT, scale bar 200  $\mu\text{m}$ .

20:50 for gellan gum to raw SWCNTs was obtained by comparing the stability of SWCNT suspensions obtained at different mass ratios. At this mass ratio, both carbonaceous impurity particles and SWCNTs absorbed gellan gum onto their surfaces, achieving stable dispersion in water and no obvious sedimentation even after high speed centrifugation treatment, as shown in Figure 1a. The low mass ratio of polymer dispersant to SWCNT will give low viscosity of suspension, which allows the preparation of highly concentrated SWCNT solution.<sup>23</sup> It is known that disordered rod-like CNTs of high aspect ratio at high concentration have been theoretically and experimentally found<sup>28</sup> to be thermodynamically unstable and have to minimize their system energy by adjusting their orientation to an aligned state, forming the CNT liquid crystal phase. However, in our experiment, no liquid crystal phase for the highly concentrated SWCNT suspensions could be detected (Figure 1b), even when we increase the period of sonication dispersion treatment, the aging time of the sample, and the concentration of SWCNTs. This contradicts that of theoretically predicted and experimentally realized results. Large amount of spherical carbonaceous impurities that coexist with the SWCNTs attracted our attention and are suspected to be an important issue that hinders achieving the SWCNT liquid crystal phase.

CNTs and carbonaceous impurities have different properties, such as thermal and chemical stability, which has been used to purify CNTs.<sup>29,30</sup> However, these purification methods are complicated and time-consuming, introduce defects onto the CNT surface, and normally produce a low yield. To obtain large amounts of pristine SWCNTs for high volume usage, such as preparation of SWCNT liquid crystal phase from highly concentrated purified SWCNT suspension, a high yield and nondestructive purification method is desired. During our experiments, we found that a large amount of spherical carbonaceous impurity particles precipitate when

the dispersant amount is insufficient to stabilize all of the SWCNTs and impurities. SWCNT appears to favor absorbing polymer gellan gum more than carbonaceous impurities do under such conditions. This phenomenon is thought to be caused by the different surface structure of SWCNTs and carbonaceous impurities, which is similar to previous reports on the separation of arc-discharge produced SWCNTs from fullerenes.<sup>31,32</sup> It gives us an easy method to effectively separate SWCNTs from carbonaceous impurities at the hundred milligram level.

To verify the purification effect, Raman spectroscopy and FESEM have been used. The D band intensity of SWCNT Raman spectra decreases when the mass ratio of gellan gum to SWCNTs decreases from 20:50 to 10:50, as shown in Figure 2. This means that the carbonaceous impurities have been largely removed from SWCNTs at the mass ratio of 10:50. Further reducing this mass ratio leads to dramatic increase in sedimentation amount, with little SWCNTs suspended. The mass ratio of 10:50 for gellan gum to raw SWCNTs is thus thought to be the most effective value to separate SWCNTs from carbonaceous impurities in our experiment. The FESEM image in Figure 3a,b shows that SWCNTs are dominant in the supernatant while carbon-

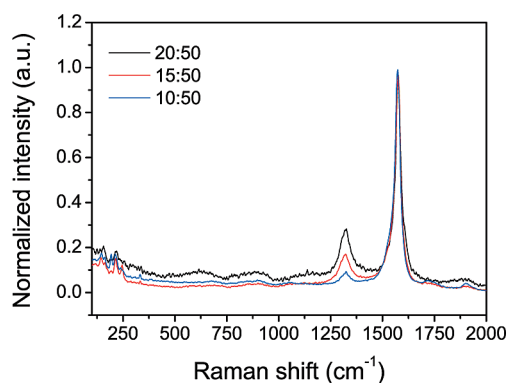


**Figure 2.** Normalized Raman spectra for dried supernatants from centrifuged SWCNT suspensions of different initial mass ratio of 20:50, 15:50, and 10:50 for gellan gum to SWCNTs.

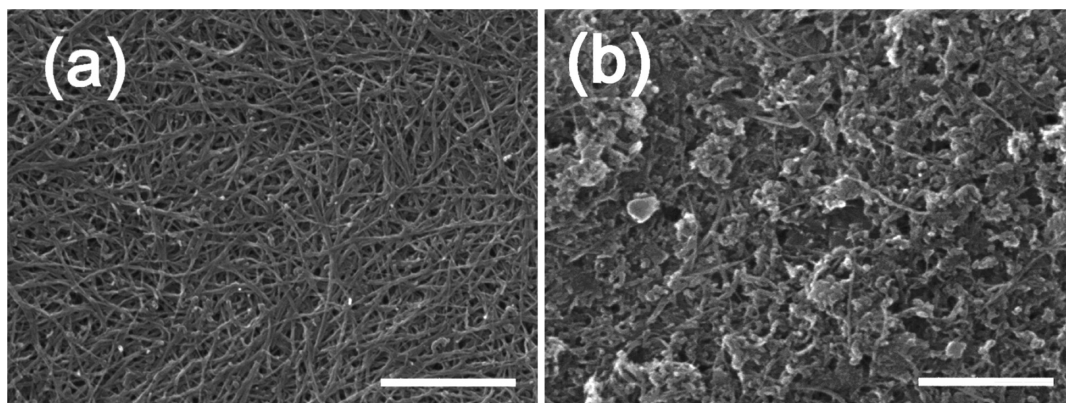


Figure 3. FESEM images for (a) the purified SWCNTs and (b) the separated impurities, scale bar 500 nm.

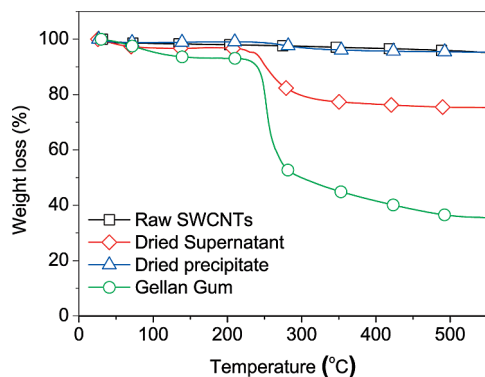


Figure 4. TGA curve for pure SWCNTs (square), dried supernatant (diamond), and precipitate (triangle) of gellan gum dispersed SWCNTs and pure gellan gum (circle).

aceous impurities are largely enriched in the precipitate.

Thermal gravimetric analysis (TGA) curves, shown in Figure 4, have been used to calculate the mass ratio of gellan gum to SWCNTs in supernatant and gellan gum to carbonaceous impurities in precipitate based on the reported method<sup>33</sup> (see Supporting Information Figure S1). The mass ratio for gellan gum to SWCNTs in supernatant is about 1:1.77. Meanwhile, the mass ratio of gellan gum to carbonaceous impurities in the precipitate is 0.04:1, which indicates that little gellan gum absorbed

onto carbonaceous impurities' surface. The calculated amount of purified SWCNTs in solution is about 46 mg in 20 mL of supernatant. The finally obtained 1 mL of highly concentrated suspension should have SWCNT concentration of 46 mg/mL.

After the purification procedure, the highly concentrated SWCNT suspensions were then obtained by carefully evaporating the collected SWCNT supernatants by a factor of 20. As shown in Figure 5, large-scale birefringence could be observed from both highly concentrated purified SWCNT suspensions and their dried solid membranes but not in pure gellan gum solution. The alignment of SWCNTs in the composite membrane has been achieved.

Direct evidence of aligned SWCNTs in the polymer matrix is shown in Figure 6a. The aligned structure was found to be dominant in the whole sample after checking a  $10 \times 10 \text{ mm}^2$  area. The orientation direction of aligned SWCNTs is randomly distributed. The size of each continuous part of certain SWCNT orientation direction in the composite membrane has been found to be above  $20 \mu\text{m}$  and normally more than  $100 \mu\text{m}$  in accordance with what is shown in Figure 5b. In addition, we investigated the alignment of SWCNTs in composite membranes that were prepared from suspensions of partly purified SWCNTs at an initial mass ratio of 15:50. The FESEM

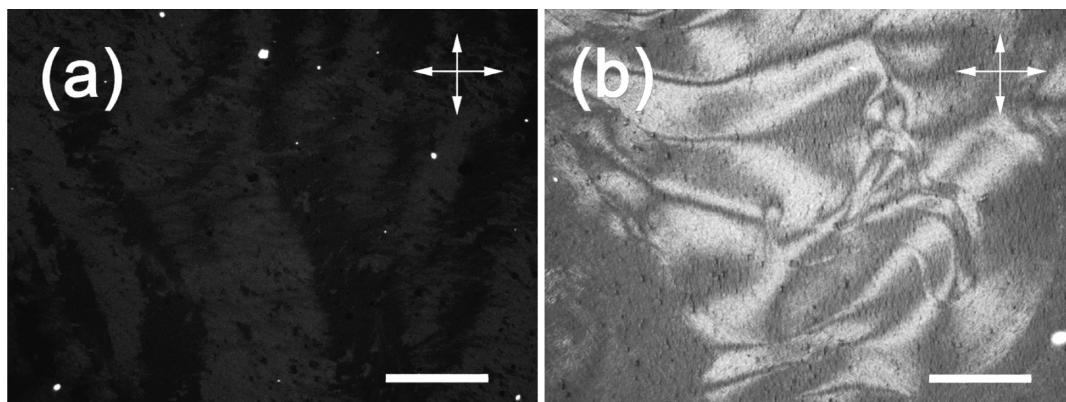


Figure 5. Polarizing microscopic images for (a) suspension and (b) solid state composite membrane between cross polarizers (scale bar  $200 \mu\text{m}$ ).

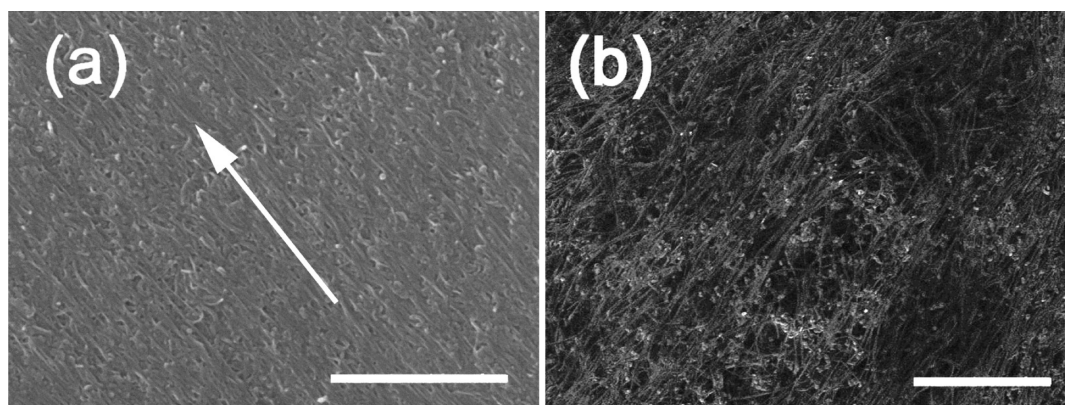


Figure 6. FESEM images for composite membranes of (a) purified SWCNTs, scale bar 500 nm, and (b) partly purified SWCNTs, scale bar 1  $\mu\text{m}$ .

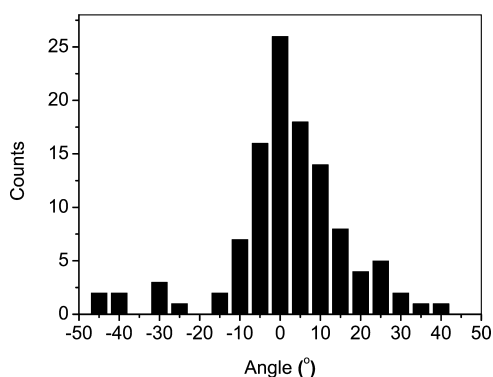


Figure 7. Angular distribution for long axes of nanotubes with respect to their optimal aligned direction in the composite membrane.

image in Figure 6b shows a micrometer size weak alignment with spherical impurities. This further proved the importance of removing spherical impurities to achieve SWCNT alignment.

The order parameter for aligned SWCNTs in the composite membrane has been calculated from high-magnification FESEM images. The order parameter for the two-dimensional system was calculated from the equation

$$S = \langle 2 \cos^2 \theta - 1 \rangle$$

The bracket indicates an average over all of the angles  $\theta$  between the optimal aligned direction and the main tube axis. The axis distribution for SWCNT/gellan gum core-shell units is shown in Figure 7. Thus, the order parameter was calculated to be 0.88.

Defects of SWCNT liquid crystal vary the orientation of aligned SWCNTs. On the boundary of each region of different SWCNT orientation, defects could be detected. The polarizing microscopic image in Figure 8a shows a typical liquid crystal defect<sup>17,34,35</sup> that was preserved in the composite membrane. This kind of defect of  $-1/2$  strength disclination could also be observed by FESEM, as shown in Figure 8b. In the center core of disclination, the entangled SWCNTs could be easily observed. Kinked SWCNTs that may form in the growth process or during the sonication treatment can also be detected between the aligned SWCNTs. These already kinked SWCNTs combined with sonication seriously shortened SWCNTs, and the residual impurities in the suspension are thought to be the cause of the defects of aligned SWCNTs.

The composite membrane prepared by simple evaporation has aligned SWCNTs in various directions of orientation. Controlling the orientation of aligned SWCNTs in one direction by shearing the liquid crystal of SWCNTs on a glass substrate in a spin coater has been done following the literature

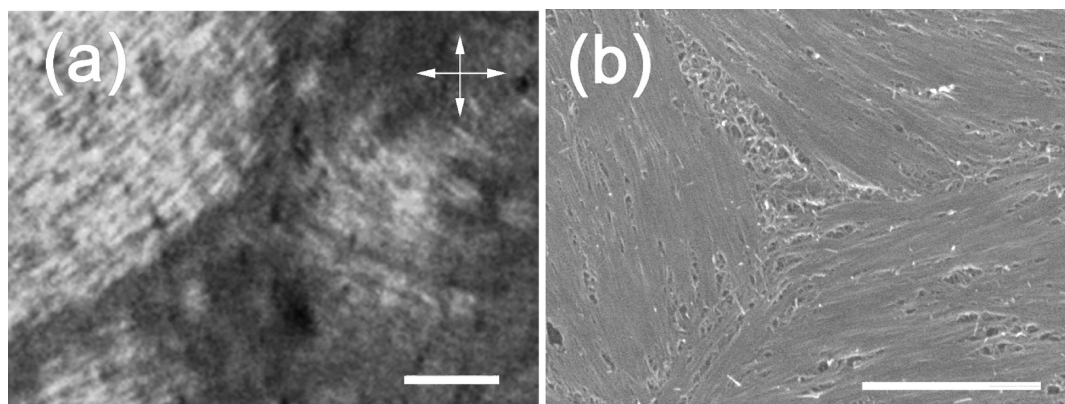


Figure 8. (a) Polarizing microscopic image of a liquid crystal defect in the composite of well-purified SWCNTs, scale bar 5  $\mu\text{m}$ ; (b) FESEM image for a liquid crystal defect, scale bar 1  $\mu\text{m}$ .

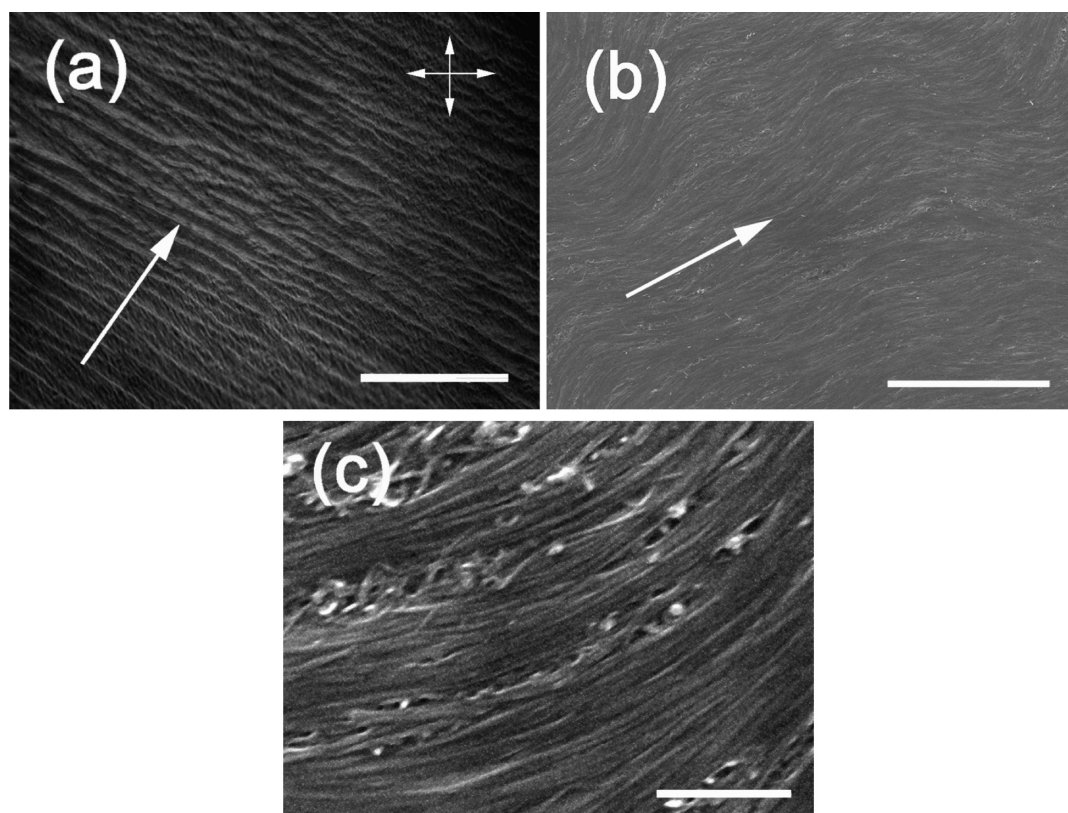


Figure 9. (a) Polarizing microscope image of the band structure observed in a sheared composite membrane (white arrow is sheared direction), scale bar 50  $\mu\text{m}$ ; (b) FESEM image showing the waviness of SWCNTs in the band structure, scale bar 3  $\mu\text{m}$ ; (c) enlarged image of wavy SWCNTs, scale bar 400 nm.

method.<sup>24</sup> The polarizing microscopic image for a sheared membrane has the band structure, as shown in Figure 9a. FESEM image in Figure 9b,c shows that SWCNTs are “wavyly” aligned along the shear direction. We have also sheared the isotropic suspension of purified SWCNTs. No obvious bireflection could be detected. This method only has an effect for the SWCNT liquid crystal phase. The anisotropic electrical performance has been characterized by a four-probe method (see Supporting Information Figure S3) for the mechanical shear controlled orientation of aligned SWCNT composite membrane of 2.5  $\mu\text{m}$  thickness.  $I$ – $V$  curves for the electric field applied parallel and perpendicular to the SWCNT aligned direction are shown in Figure 10. In the parallel direction, the composite membrane has a much lower potential fall at a given voltage than that of the perpendicular direction, which embodied the macroscopic anisotropic electrical resistivity of the sheared composite membrane. The calculated resistivity in the parallel direction is as low as  $1.477 \times 10^{-4} \Omega\text{m}$ .

## CONCLUSION

In summary, the removal of spherical impurities from SWCNTs has been shown to be very important for achieving SWCNT alignment, which has been achieved by an effective physical purification method. Benefiting from an extremely easy and nondestructive

purification method and low mass ratio of gellan gum to SWCNTs, highly concentrated purified SWCNT suspensions were obtained and used to form a SWCNT liquid crystal phase. Large-scale aligned SWCNTs in a solid composite membrane were thus initially obtained by simple shearing of the SWCNT liquid crystal, showing anisotropic electrical performance. Further work is ongoing to improve the alignment of SWCNTs in composite materials with a view for potential uses in high-performance SWCNT biocomposite functional materials such as sensors and actuators.

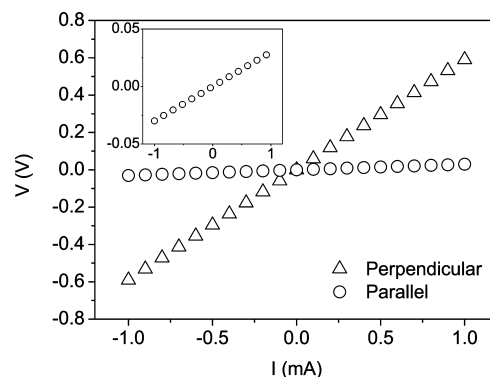


Figure 10.  $I$ – $V$  curves for the electric field applied perpendicular and parallel to the sheared direction of composite membrane; inset is the enlarged image for the curve of electric perpendicular to that of the shear direction.

## EXPERIMENTAL SECTION

**Materials.** Disordered SWCNTs prepared by chemical vapor deposition method (SWCNTs >50 wt %, average diameter <2 nm, length 5–15  $\mu\text{m}$ , carbonaceous impurities <47 wt %, and metal catalyst <3 wt %) were obtained from Shenzhen Nanotech Port Co. Ltd., and gellan gum (purity 87.5 wt %, water 12.5 wt %, average molecular weight about 500 kDa) obtained from Hebei Xinhe Biochemical Co. Ltd. was used as received.

**Method.** SWCNT suspensions were typically prepared as follows: 20 mg of gellan gum was added to 20 mL of deionized water (resistivity = 18.4 M $\Omega\text{cm}$ ). The mixture was stirred at 60 °C in a water bath for 30 min to obtain a homogeneous solution. Then, 100 mg of as-received SWCNTs was added into the gellan gum solution and sonicated with a sonicator horn for 15 min (accumulated sonication time) in an ice–water bath in a program of 0.5 s on and 2 s off at a 20 W and 20 kHz frequency output. To accelerate the precipitation of unstable suspended particles, 15 min high speed centrifugation (10 000g) was used at room temperature after the suspension aged overnight. The volume of collected supernatant was adjusted to 20 mL by adding deionized water. Other suspensions of different mass ratios of gellan gum to SWCNTs were prepared by changing the added gellan gum amounts. Highly concentrated SWCNT suspensions of 5 mL were prepared by carefully evaporating 100 mL of collected as-purified SWCNT suspensions by a factor of 20.

Liquid crystal samples for polarizing microscopy analysis were prepared by injecting highly concentrated SWCNT suspensions into concave dimples of slides. Glass covers were carefully placed onto the concave dimples and sealed with gel to prevent evaporation. The concentrated samples used to form liquid crystal phase were placed at room temperature for 2 weeks before characterization. For purification characterization, the solid samples were prepared by evaporating the SWCNT suspension 24 h after been prepared. Solid membrane samples for Raman spectra, field emission scanning electron microscope, and polarizing microscopic characterization were prepared by drying SWCNT suspensions on a glass substrate at 70 °C for one night. Samples of controlled SWCNT aligned direction were prepared as follows: a droplet of suspension was first placed on a glass substrate that was fixed in a spin coater and then an upper flat substrate approached the surface of the viscous suspension during the rotation. The suspension solidified in several seconds after being sheared and was further dehydrated at 70 °C overnight. Samples for thermogravimetric analysis characterization were prepared by drying the as-purified SWCNT suspension on Teflon dishes at 70 °C for one night to remove most of the water. The weight was recorded for required calculations. About 2 mg of the solid samples was transported into a Pt pan in N<sub>2</sub> gas flow and 10 °C/min temperature raising program for TGA characterization. All substrates and containers we used were repeatedly cleaned by ethanol and deionized water. Glass substrates were further cleaned by plasma oxidation to remove organic residuals on the substrate surface and preserved for experiment use.

**Equipment.** Sonication was processed using a Fisher Scientific model 500 digital sonic dismembrator equipped with a 12.5 mm diameter disruptor horn. TGA was performed with Seiko TG/DTA 6300 instruments. Bireflection microscopic images were recorded using a Leica BM400 polarizing microscope. The images are in reflected polarized light with the poles crossed (bireflection). Field emission scanning electron microscopy images were recorded using a FEI Quanta400FEG. Transmission electron microscope (TEM) images were recorded using a Tecnai G2 F20 S-TWIN at 200 kV. Raman spectra were collected using a Jobin-Yvon LabRam HR 800 confocal micro-Raman system, equipped with an electrical-cooled detector. Excitation wavelength is 632.8 nm with a He–Ne laser. Electrical performance measurement was carried out in Agilent B1500A semiconductor device analyzer.

**Acknowledgment.** We wish to thank National Natural Science Foundation of China (10704051), Science and Technology Program of Suzhou (ZXG0713), and the Characterization Platform of Suzhou Institute of Nanotech and Nanobionics, Chinese Academy of Sciences.

**Supporting Information Available:** Details for mass ratio calculation from TGA curves, TEM image and length distribution of gellan gum dispersed SWCNTs and electrical characterization of

anisotropic composite membrane. This material is available free of charge via the Internet at <http://pubs.acs.org>.

## REFERENCES AND NOTES

- Ren, Z. F.; Huang, Z. P.; Xu, J. W.; Wang, J. H.; Bush, P.; Siegal, M. P.; Provencio, P. N. Synthesis of Large Arrays of Well-Aligned Carbon Nanotubes on Glass. *Science* **1998**, *282*, 1105–1107.
- Thong, J. T. L.; Oon, C. H.; Eng, W. K.; Zhang, W. D.; Gan, L. M. High-Current Field Emission from a Vertically Aligned Carbon Nanotube Field Emitter Array. *Appl. Phys. Lett.* **2001**, *79*, 2811–2813.
- Javey, A.; Wang, Q.; Ural, A.; Li, Y. M.; Dai, H. J. Carbon Nanotube Transistor Arrays for Multistage Complementary Logic and Ring Oscillators. *Nano Lett.* **2002**, *2*, 929–932.
- Jin, L.; Bower, C.; Zhou, O. Alignment of Carbon Nanotubes in a Polymer Matrix by Mechanical Stretching. *Appl. Phys. Lett.* **1998**, *73*, 1197–1199.
- Haggenmuller, R.; Gommans, H. H.; Rinzler, A. G.; Fischer, J. E.; Winey, K. I. Aligned Single-Wall Carbon Nanotubes in Composites by Melt Processing Methods. *Chem. Phys. Lett.* **2000**, *330*, 219–225.
- Safadi, B.; Andrews, R.; Grulke, E. A. Multiwalled Carbon Nanotube Polymer Composites: Synthesis and Characterization of Thin Films. *J. Appl. Polym. Sci.* **2002**, *84*, 2660–2669.
- De Heer, W. A.; Bacsá, W. S.; Chatelain, A.; Gerfin, T.; Humphrey-Baker, R.; Forro, L.; Ugarte, D. Aligned Carbon Nanotube Films: Production and Optical and Electronic Properties. *Science* **1995**, *268*, 845–847.
- Casavant, M. J.; Walters, D. A.; Schmidt, J. J.; Smalley, R. E. Neat Macroscopic Membranes of Aligned Carbon Nanotubes. *J. Appl. Phys.* **2003**, *93*, 2153–2156.
- Vigolo, B.; Penicaud, A.; Coulon, C.; Sauder, C.; Paillet, R.; Journet, C.; Bernier, P.; Poulin, P. Macroscopic Fibers and Ribbons of Oriented Carbon Nanotubes. *Science* **2000**, *290*, 1331–1334.
- Chen, W.; Tao, X. M. Self-Organizing Alignment of Carbon Nanotubes in Thermoplastic Polyurethane. *Macromol. Rapid Commun.* **2005**, *26*, 1763–1767.
- Zhang, M.; Smith, A.; Gorski, W. Carbon Nanotube–Chitosan System for Electrochemical Sensing Based on Dehydrogenase Enzymes. *Anal. Chem.* **2004**, *76*, 5045–5050.
- Sotiropoulou, S.; Chaniotakis, N. A. Carbon Nanotube Array-Based Biosensor. *Anal. Bioanal. Chem.* **2003**, *375*, 103–105.
- Baughman, R. H.; Cui, C. X.; Zakhidov, A. A.; Iqbal, Z.; Barisci, J. N.; Spinks, G. M.; Wallace, G. G.; Mazzoldi, A.; Rossi, D. D.; Rinzler, A. G.; Jaschinski, O.; Roth, S.; Kertesz, M. Carbon Nanotube Actuators. *Science* **1999**, *284*, 1340–1344.
- Zhang, M. G.; Gorski, W. Electrochemical Sensing Platform Based on the Carbon Nanotubes/Redox Mediators–Biopolymer System. *J. Am. Chem. Soc.* **2005**, *127*, 2058–2059.
- Aliev, A. E.; Oh, J. Y.; Kozlov, M. E.; Kuznetsov, A. A.; Fang, S. L.; Fonseca, A. F.; Ovalle, R.; Lima, M. D.; Haque, M. H.; Gartstein, Y. N.; Zhang, M.; Zakhidov, A. A.; Baughman, R. H. Giant-Stroke, Superelastic Carbon Nanotube Aerogel Muscles. *Science* **2009**, *323*, 1575–1578.
- Whitten, P. G.; Gestos, A. A.; Spinks, G. M.; Gilmore, K. J.; Wallace, G. G. Free Standing Carbon Nanotube Composite Bio-Electrodes. *J. Biomed. Mater. Res. B*, *82*, 37–43.
- Song, W. H.; Kinloch, I. A.; Windle, A. H. Nematic Liquid Crystallinity of Multiwall Carbon Nanotubes. *Science* **2003**, *302*, 1363.
- Davis, V. A.; Ericson, L. M.; Parra-Vasquez, A. N.; Fan, H.; Wang, Y. H.; Prieto, V.; Longoria, J. A.; Ramesh, S.; Saini, R. K.; Kittrell, C.; Billups, W. E.; Adams, W. W.; Hauge, R. H.; Smalley, R. E.; Pasquali, M. Phase Behavior and Rheology of SWNTs in Superacids. *Macromolecules* **2004**, *37*, 154–160.
- Ericson, L. M.; Fan, H.; Peng, H. Q.; Davis, V. A.; Zhou, W.; Sulpizio, J.; Wang, Y. H.; Booker, R.; Vavro, J.; Guthy, C.; Parra-Vasquez, A. N.; Kim, M. J.; Ramesh, S.; Saini, R. K.

- Kittrell, C.; Lavin, G.; Schmidt, H.; Adams, W. W.; Billups, W. E.; Pasquali, M.; Hwang, W. F.; Hauge, R. H.; Fischer, J. E.; Smalley, R. E. Macroscopic, Neat, Single-Walled Carbon Nanotube Fibers. *Science* **2004**, *305*, 1447–1450.
20. Zheng, M.; Jagota, A.; Semke, E. D.; Diner, B. A.; Mclean, R. S.; Lustig, S. R.; Richardson, R. E.; Tassi, N. G. DNA-Assisted Dispersion and Separation of Carbon Nanotubes. *Nat. Mater.* **2003**, *2*, 338–342.
  21. Lynam, C.; Moulton, S. E.; Wallace, G. G. Carbon-Nanotube Biofibers. *Adv. Mater.* **2007**, *19*, 1244–1248.
  22. Badaire, S.; Zakri, C.; Maugey, M.; Derre, A.; Barisci, J. N.; Wallace, G. G.; Poulin, P. Liquid Crystal of DNA Stabilized Carbon Nanotubes. *Adv. Mater.* **2005**, *17*, 1673–1676.
  23. Moulton, S. E.; Maugey, M.; Poulin, P.; Wallace, G. G. Liquid Crystal Behavior of Single-Walled Carbon Nanotubes Dispersed in Biological Hyaluronic Acid Solutions. *J. Am. Chem. Soc.* **2007**, *129*, 9452–9457.
  24. Zamora-Ledezma, C.; Blanc, C.; Maugey, M.; Zakri, C.; Poulin, P.; Anglaret, E. Anisotropic Thin Films of Single-Wall Carbon Nanotubes from Aligned Lyotropic Nematic Suspensions. *Nano Lett.* **2008**, *8*, 4103–4107.
  25. Zhang, S. J.; Kinloch, I. A.; Windle, A. H. Mesogenicity Drives Fractionation in Lyotropic Aqueous Suspensions of Multiwall Carbon Nanotubes. *Nano Lett.* **2006**, *6*, 568–572.
  26. Panhuis, M.; Heurtematte, A.; Small, W. R.; Paunov, V. N. Inkjet Printed Water Sensitive Transparent Films from Natural Gum-Carbon Nanotube Composites. *Soft Matter* **2007**, *3*, 840–843.
  27. Islam, M. F.; Rojas, E. D.; Bergey, M.; Johnson, A. T.; Yodh, A. G. High Weight Fraction Surfactant Solubilization of Single-Wall Carbon Nanotubes in Water. *Nano Lett.* **2003**, *3*, 269–273.
  28. Zhang, S. Y.; Kumar, S. Carbon Nanotubes as Liquid Crystals. *Small* **2008**, *4*, 1270–1283.
  29. Huang, W.; Wang, Y.; Luo, G. H.; Wei, F. 99.9% Purity Multi-Walled Carbon Nanotubes by Vacuum High-Temperature Annealing. *Carbon* **2003**, *41*, 2585–2590.
  30. Furtado, C. A.; Kim, U. J.; Gutierrez, H. R.; Pan, Ling.; Dickey, E. C.; Eklund, P. C. Debundling and Dissolution of Single-Walled Carbon Nanotubes in Amide Solvents. *J. Am. Chem. Soc.* **2004**, *126*, 6095–6105.
  31. Tohji, K.; Takahashi, H.; Shinoda, Y.; Shimizu, N.; Jeyadevan, B.; Matsuoka, I.; Saito, Y.; Kasuya, A.; Ito, S.; Nishina, Y. Purification Procedure for Single-Walled Nanotubes. *J. Phys. Chem. B* **1997**, *101*, 1974–1978.
  32. Montoro, L. A.; Rosolen, J. M. A Multi-Step Treatment to Effective Purification of Single-Walled Carbon Nanotubes. *Carbon* **2006**, *44*, 3293–3301.
  33. Xue, C. H.; Shi, M. M.; Yan, Q. X.; Shao, Z.; Gao, Y.; Wu, G.; Zhang, X. B.; Yang, Y.; Chen, H. Z.; Wang, M. Preparation of Water-Soluble Multi-Walled Carbon Nanotubes by Polymer Dispersant Assisted Exfoliation. *Nanotechnology* **2008**, *19*, 115605.
  34. Cladis, P. E. Symmetries and Defects in Liquid Crystals: Arceau-Tetrahedra-Arceau. *C. R. Chimie* **2008**, *11*, 207–211.
  35. Song, W. H.; Windle, A. H. Isotropic-Nematic Phase Transition of Dispersions of Multiwall Carbon Nanotubes. *Macromolecules* **2005**, *38*, 6181–6188.